

## EPISODIC ACCRETION AT EARLY STAGES OF EVOLUTION OF LOW-MASS STARS AND BROWN DWARFS: A SOLUTION FOR THE OBSERVED LUMINOSITY SPREAD IN H–R DIAGRAMS?

I. BARAFFE<sup>1</sup>, G. CHABRIER<sup>1</sup>, AND J. GALLARDO<sup>2</sup>

<sup>1</sup> École Normale Supérieure, Lyon, CRAL (UMR CNRS 5574), Université de Lyon, France; [ibaraffe@ens-lyon.fr](mailto:ibaraffe@ens-lyon.fr), [chabrier@ens-lyon.fr](mailto:chabrier@ens-lyon.fr)

<sup>2</sup> Observatorio Astronómico Cerro Calán, Departamento de Astronomía, Universidad de Chile, Casilla 36-D Santiago, Chile; [gallardo@das.uchile.cl](mailto:gallardo@das.uchile.cl)

Received 2009 May 22; accepted 2009 July 17; published 2009 August 13

### ABSTRACT

We present evolutionary models for young low-mass stars and brown dwarfs taking into account episodic phases of accretion at early stages of the evolution, a scenario supported by recent large surveys of embedded protostars. An evolution including short episodes of vigorous accretion ( $\dot{M} \geq 10^{-4} M_{\odot} \text{ yr}^{-1}$ ) followed by longer quiescent phases ( $\dot{M} < 10^{-6} M_{\odot} \text{ yr}^{-1}$ ) can explain the observed luminosity spread in H–R diagrams of star-forming regions at ages of a few Myr, for objects ranging from a few Jupiter masses to a few tenths of a solar mass. The gravitational contraction of these accreting objects strongly departs from the standard Hayashi track at constant  $T_{\text{eff}}$ . The best agreement with the observed luminosity scatter is obtained if most of the accretion shock energy is radiated away. The obtained luminosity spread at 1 Myr in the H–R diagram is equivalent to what can be misinterpreted as an  $\sim 10$  Myr age spread for non-accreting objects. We also predict a significant spread in radius at a given  $T_{\text{eff}}$ , as suggested by recent observations. These calculations bear important consequences for our understanding of star formation and early stages of evolution and on the determination of the initial mass function for young ( $\leq$  a few Myr) clusters. Our results also show that the concept of a stellar birthline for low-mass objects has no valid support.

*Key words:* accretion, accretion disks – stars: formation – stars: low-mass, brown dwarfs

### 1. INTRODUCTION

The significant luminosity spread observed in Hertzsprung–Russell (H–R) diagrams of star-forming regions (SFRs) and young clusters is a well known feature, which has been confirmed with the improvement of observational techniques (see Hillenbrand 2009 and references therein). Whether this luminosity spread arises from a physical process, observational uncertainties, or reveals a significant age spread is a crucial question, with important consequences for our understanding of star formation (Hartmann 2001). This hypothetical age spread is used as an argument in favor of a slow star formation process, in conflict with other observational constraints and our current understanding of star formation (Hartmann 2001; Ballesteros-Paredes & Hartmann 2007). Motivated by this controversy, we have conducted a systematic analysis of how accretion affects the evolution of young low-mass stars (LMS) and brown dwarfs (BDs) in order to explore the sensitivity of evolutionary tracks to the early accretion history. In this Letter, we present the first consistent evolutionary models for young LMS and BDs taking into account non-steady accretion phases at very early stages of the evolution. We show that this scenario can explain, at least partly, the observed luminosity spread in H–R diagrams, without invoking an age spread.

Current observational analysis of embedded protostars strongly suggests that accretion onto forming stars must be transient, with very large fluctuations (Dunham et al. 2008; Enoch et al. 2009; Evans et al. 2009). Enoch et al. (2009) find in three clouds a large population of low-luminosity class I sources that aggravate the well known “luminosity problem” (Kenyon et al. 1990). Long quiescent phases of accretion ( $\dot{M} \lesssim 10^{-6} M_{\odot} \text{ yr}^{-1}$ ) interrupted by short episodes of high accretion ( $\dot{M} \gtrsim 10^{-5} M_{\odot} \text{ yr}^{-1}$ ) provide a consistent picture explaining both the large population of low-luminosity class I sources and the small fraction of very luminous sources. Enoch et al. (2009) also rule out drastic changes in the accretion rates

from class 0 to class I, and in particular the standard picture of short ( $\sim 10^4$  yr) class 0 duration.<sup>3</sup> Evans et al. (2009) suggest that a star could assemble half its mass during a few episodes of high accretion, occurring throughout about 7% of the class I lifetime. The idea of non-steady, time-varying accretion rates is not new, since for decades FU Ori objects have been providing evidence for short episodes of rapid accretion at early stages of evolution, with rates much larger than the aforementioned typical class 0 infall rates for low-mass objects (Kenyon & Hartmann 1995).

The calculations presented in this Letter are a theoretical formulation of such an evolution including phases of episodic accretion for proto- or young LMS and BDs. In Section 2, we briefly summarize the evolutionary models and the treatment of accretion; details will be presented in a forthcoming paper (Gallardo et al. 2009). Results and comparison with observations are presented in Section 3, followed by discussion and conclusion in Section 4.

### 2. EVOLUTIONARY MODELS AND TREATMENT OF ACCRETION

The evolutionary calculations for LMS and BDs are based on the Lyon stellar evolution code with input physics described in Chabrier & Baraffe (1997) and Baraffe et al. (1998). The treatment of accretion is based on a simplified one-dimensional approach, adopting similar assumptions and simplifications as Hartmann et al. (1997) and Siess et al. (1997). We assume that accretion onto the central object rapidly proceeds non-spherically, affecting only a small fraction  $\delta$  of the contracting object’s surface. The object can thus freely radiate its energy over most of its photosphere (see Hartmann et al. 1997 and references therein). The accreting material brings, per unit mass, a gravitational energy  $-GM/R$  and an internal energy

<sup>3</sup> Standard estimates for ages and rates are  $\sim 10^4$  yr and  $\dot{M} \sim 10^{-5} M_{\odot} \text{ yr}^{-1}$  for class 0 and  $\sim 10^5$  yr and  $\dot{M} \sim 10^{-6} M_{\odot} \text{ yr}^{-1}$  for class I sources.

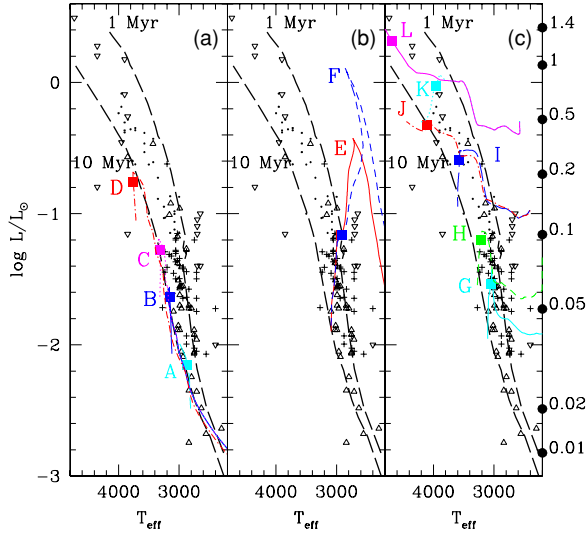


**Figure 1.** Effect of accretion on the evolution in a HR diagram for objects with different initial masses  $m_i$ . The two long dashed (black) curves are the 1 Myr and 10 Myr isochrones of Baraffe et al. (1998) for non-accreting models. The solid (black) circles on the rightmost Y-axis give the luminosity of non-accreting models at 1 Myr for the indicated masses (in  $M_\odot$ ). The colored curves show calculations for various accretion rates described in Table 1. The solid squares on each curve give the position at 1 Myr. (a) Initial mass  $m_i = 1M_{\text{Jup}}$  and  $\alpha = 0$ . (b) Initial mass  $m_i = 1M_{\text{Jup}}$  and  $\alpha \neq 0$ . Note that both sequences reach the same location at 1 Myr. (c) Initial masses  $m_i > 1M_{\text{Jup}}$ . Other symbols are observations in SFRs ( $\nabla$  Gatti et al. 2006;  $\cdot$  Gatti et al. 2008;  $+$  Peterson et al. 2008;  $\Delta$  Muzerolle et al. 2005).

$+\epsilon GM/R$ , i.e., an energy rate:

$$\frac{dE_{\text{acc}}}{dt} = (\epsilon - 1) \frac{GM\dot{M}}{R}. \quad (1)$$

The value of  $\epsilon$  depends on the details of the accretion process, with  $\epsilon \leq 1$  for gravitationally bound material and  $\epsilon \leq \frac{1}{2}$  if gas accretes from a thin disk at the object's equator (Hartmann et al. 1997). We denote  $\alpha$  ( $\alpha \leq 1$ ) the fraction of accreting internal energy absorbed by the proto-star/BD, which thus contributes to its heat content. The total additional energy rate gained by the accreting object and the accreting luminosity radiated away thus read, respectively, for  $\delta \ll 1$  (see, e.g., Hartmann et al. 1997):

$$L_{\text{add}} = \alpha\epsilon \frac{GM\dot{M}}{R}; \quad L_{\text{acc}} = \epsilon(1 - \alpha) \frac{GM\dot{M}}{R}. \quad (2)$$

The case  $\alpha \ll 1$  corresponds to accreted matter arriving on the object's surface with a lower specific entropy than that of the object.

### 3. RESULTS

#### 3.1. Exploring Accretion Rates

We have conducted evolutionary calculations taking into account the effect of accretion on proto low-mass objects for a wide range of initial proto-star/BD masses from  $10^{-3}M_\odot$  ( $\sim 1M_{\text{Jup}}$ ) to  $0.1M_\odot$ , with arbitrary large initial radii between  $\sim 1R_\odot$  and  $\sim 4R_\odot$ . The results are compared to recent surveys of LMS and BDs between  $\sim 0.01M_\odot$  and  $1M_\odot$  in various SFRs, with characteristic ages of a few Myr, namely Taurus and Chamaeleon I (Muzerolle et al. 2005),  $\rho$  Ophiucus (Gatti et al. 2006), Orion molecular cloud (Peterson et al. 2008), and  $\sigma$ -Orionis (Gatti et al. 2008). Given the loose constraints

**Table 1**  
Parameters of the Evolutionary Sequences Shown in Figure 1

Case	$m_i$	$m_f$	$T_{\text{eff}1}$	$L_1$	$T_{\text{eff}}^{\text{BCAH98}}$	$L^{\text{BCAH98}}$	$\dot{M}$	$\Delta t$	$\alpha$
A	1	0.05	2860	-2.15	2844	-1.73	$10^{-5}$	$5 \times 10^3$	0
B	1	0.1	3157	-1.63	3001	-1.16	$10^{-5}$	$10^4$	0
C	1	0.2	3320	-1.27	3193	-0.69	$10^{-5}$	$2 \times 10^4$	0
D	1	0.5	3756	-0.75	3426	-0.28	$5 \times 10^{-5}$	$10^4$	0
E	1	0.1	3000	-1.16	3001	-1.16	$10^{-5}$	$10^4$	0.2
F	1	0.1	2998	-1.16	3001	-1.16	$10^{-5}$	$10^4$	1
G	5	0.1	3051	-1.53	3001	-1.16	$10^{-5}$	$10^4$	0
H	10	0.21	3221	-1.20	3201	-0.67	$10^{-5}$	$2 \times 10^4$	0
I	50	0.55	3571	-0.59	3468	-0.22	$10^{-5}$	$5 \times 10^4$	0
J	50	1.05	4102	-0.32	3840	0.17	$5 \times 10^{-5}$	$2 \times 10^4$	0
K	100	1.1	3961	-0.03	3870	0.20	$5 \times 10^{-5}$	$2 \times 10^4$	0
L	100	1.85	4677	0.31	4377	0.60	$5 \times 10^{-5}$	$3.5 \times 10^4$	0

**Notes.**  $m_i$  and  $m_f$  are respectively the initial (in  $M_{\text{Jup}}$ ) and final (in  $M_\odot$ ) masses,  $T_{\text{eff}1}$  and  $L_1$  the effective temperature and log of the luminosity (in units of  $L_\odot$ ) respectively at 1 Myr,  $T_{\text{eff}}^{\text{BCAH98}}$  and  $L^{\text{BCAH98}}$  the values predicted by the BCAH98 (non-accreting) models for the mass  $m_f$  at 1 Myr,  $\dot{M}$  the accretion rate (in  $M_\odot \text{ yr}^{-1}$ ) applied during a time  $\Delta t$  (in yr), and  $\alpha$  the fraction of accretion energy absorbed by the object (assuming  $\epsilon=1/2$ , see text).

on accretion rates at early times, during the class 0 and class I embedded phases, we have explored a wide range of mass accretion rates and time dependences, and considered different values of  $\alpha$ . We have considered (1) constant rates, (2) exponentially time-decreasing rates, and (3) rates obeying the empirical mass dependence  $\dot{M} \propto M^2$  observed in young clusters (Mohanty et al. 2005; Herczeg & Hillenbrand 2008). The strong constraint of our calculations is to be consistent with the observed rate determinations at an age of a few Myr.

We find that assuming initial accretion rates  $\sim 10^{-6}M_\odot \text{ yr}^{-1}$ , as traditionally used in protostellar evolutionary models (Myers et al. 1998; Young & Evans 2005), produces too small a luminosity scatter in H-R diagrams after a few Myr to explain the observed spread. More severe effects are obtained when adopting higher accretion rates,  $\dot{M} \sim (1-5) \times 10^{-5}M_\odot \text{ yr}^{-1}$ , during the first few  $10^3$  to  $10^4$  years of evolution, depending on the mass. Figure 1 shows the effect of such high early accretion rates on the evolution of low-mass objects for different initial masses  $m_i$ . Evolution proceeds as time increases from the right to the left part of the H-R diagram for a given track. The tracks of the accreting objects are displayed up to an age of 10 Myr with the locations at 1 Myr indicated by the solid squares. The evolutionary sequences start from large initial radii and thus with short thermal timescales,  $\tau_{\text{KH}} \approx \frac{GM^2}{RL} \sim 10^3 \text{ yr}$ , of the order of or less than the accretion timescale  $\tau_{\text{acc}} \sim M/\dot{M}$ . Consequently, variations of the initial radius by a factor 2–3 have no significant effect on the overall evolution, barely changing the final location at 1 Myr. The parameters of the various sequences are given in Table 1.

For  $\alpha = 0$ , i.e., if all the accreting energy is radiated away, the aforementioned high accretion rates yield significantly smaller radii than those of non-accreting objects of same mass and age. This stems from the fact that, as mass builds up, the object's thermal timescale  $\tau_{\text{KH}}$  rapidly increases, and becomes much longer than the accreting timescale  $\tau_{\text{acc}}$ , so that rapid increase of gravitational energy is the only possibility of adjusting to the accreting energy flow. For example, the case B sequence (the solid blue line in Figures 1(a) and 2) starts its evolution with  $m_i = 1M_{\text{Jup}}$  and  $\tau_{\text{KH}} \sim 10^3 \text{ yr}$ . At  $10^4 \text{ yr}$ , when accretion is arbitrarily stopped, the object has a mass of  $0.1M_\odot$ , a radius of

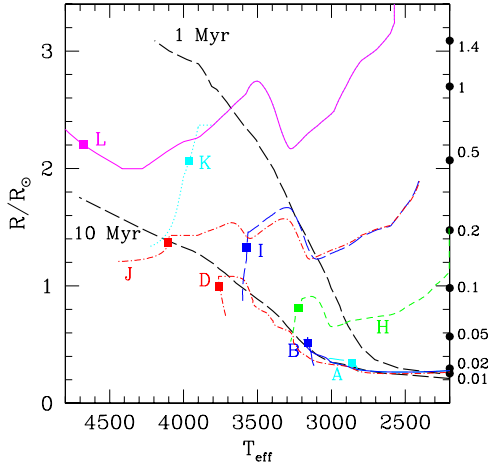


**Figure 2.** Evolution of the radius versus  $T_{\text{eff}}$  for accreting objects of different initial masses. The colored curves correspond to different accretion sequences described in Table 1. The other curves and symbols are the same as in Figure 1. The solid (black) circles on the rightmost Y-axis give the radius of non-accreting models at 1 Myr for the indicated masses (in  $M_{\odot}$ ).

$\sim 0.5 R_{\odot}$ , a luminosity of  $L \sim 2.5 \times 10^{-2} L_{\odot}$ , and a thermal timescale of  $\tau_{\text{KH}} \sim 2 \times 10^7$  yr. Similar results are obtained for all the other sequences starting from larger initial masses. The radius of these accreting objects is thus already smaller after a few  $10^4$  yr than that of the non-accreting counterparts of same mass at an age of 1 Myr (see Figure 2). The objects will eventually slowly contract toward their location on the H–R diagram at 1 Myr after the high accretion phase has been stopped, looking much fainter than the non-accreting 1 Myr old objects (see Figure 1). The spread in luminosity obtained in Figure 1 thus essentially reflects a spread in radius, as illustrated in Figure 2. Note that we find similar results if we apply smaller, non-zero accretion rates,  $\dot{M} \lesssim 10^{-6} M_{\odot} \text{ yr}^{-1}$ , after the strong accretion phase, while fulfilling the condition to recover typical observed rates at  $\sim 1$  Myr.

For the case  $\alpha \neq 0$ , i.e., if some fraction of the accretion energy contributes to the proto-star/BD thermal content, the spread at 1 Myr is smaller than for the  $\alpha = 0$  case. Assuming  $\epsilon = 1/2$  in Equation (2), characteristic of accretion from a thin disk (see Section 2), we find that for  $\alpha \lesssim 0.2$  the contraction of the structure due to mass accretion is partly compensated by this energy input, yielding a less drastic contraction. The objects are still slightly fainter at  $\sim 1$  Myr than their non-accreting counterparts, but the effect is not as significant as in the  $\alpha = 0$  case. For  $\alpha \gtrsim 0.2$ , the effect of the extra accreting energy contribution to the protostar heat content becomes dominant and the evolution now mostly proceeds at higher luminosity (see Figure 1(b)) and larger radius than for non-accreting objects. This in turn implies *shorter* thermal timescales, so that once high accretion rates are stopped or significantly decreased to recover the observed values at  $\sim 1$  Myr, the object quickly contracts and reaches a position at 1 Myr in the H–R diagram very close to the non-accreting location. In order to maintain a high luminosity and radius after  $\sim 1$  Myr, i.e., a location in the H–R diagram *above* the 1 Myr non-accreting isochrone, too large accretion rates (and large values of  $\alpha$ ) have to be maintained, inconsistent with observations of class II objects at this age.

### 3.2. Episodic Accretion

The exploratory analysis presented in the previous section demonstrates that the early accretion history still significantly

**Table 2**  
Parameters of the Evolutionary Sequences Assuming Episodic Accretion and Shown in Figure 3

Case	$m_i$	$m_f$	$T_{\text{eff}1}$	$L_1$	$T_{\text{eff}}^{\text{BCAH98}}$	$L^{\text{BCAH98}}$	$\dot{M}_{\text{burst}}$	$\Delta t_{\text{quiet}}$	$N_{\text{burst}}$
1a	1	0.1	3151	-2.00	3001	-1.16	$10^{-4}$	1	10
1b	1	0.2	3373	-1.25	3193	-0.69	$10^{-4}$	1	10
2b	1	0.41	3650	-0.90	3384	-0.46	$10^{-4}$	1	30
3b	10	0.38	3466	-1.05	3335	-0.43	$10^{-4}$	1	30
4a	10	0.05	2833	-1.77	2844	-1.73	$10^{-5}$	5	50
5a	50	1.35	4379	-0.16	4152	0.37	$10^{-4}$	1	150
6a	100	1.16	4039	0.00	3924	0.23	$3 \times 10^{-4}$	1	40
7a	100	1.67	4482	0.19	4317	0.53	$3 \times 10^{-4}$	1	60

**Notes.**  $m_i$ ,  $m_f$ ,  $T_{\text{eff}1}$ ,  $L_1$ ,  $T_{\text{eff}}^{\text{BCAH98}}$ , and  $L^{\text{BCAH98}}$  have the same meaning as in Table 1.  $\dot{M}_{\text{burst}}$  is the accretion rate during the bursts (in  $M_{\odot} \text{ yr}^{-1}$ ),  $\Delta t_{\text{quiet}}$  the quiescent phase duration (in units of  $10^3$  yr), and  $N_{\text{burst}}$  the total number of bursts. In all calculations, the burst duration varies between  $\sim 75$  and  $\sim 100$  years. The label “a” or “b” indicates whether the bursts start at the beginning of evolution (case (a)) or after a first phase of constant accretion ( $\dot{M} = 10^{-5} M_{\odot} \text{ yr}^{-1}$  during  $\Delta t = 10^4$  yr), as suggested by Vorobyov & Basu (2005) (case (b)).

affects the evolution of contracting objects after a few Myr. In this section, we show that the effects of accretion are similar, whether the object accretes *continuously* an amount of mass  $\Delta M$  at a constant rate  $\dot{M} \sim 10^{-5} M_{\odot} \text{ yr}^{-1}$  during  $\Delta t \sim 10^4$  yr, as examined in Section 3.1, or whether it accretes the same amount of mass during a *succession of short episodes* of high accretion rates,  $\dot{M} \geq 10^{-4} M_{\odot} \text{ yr}^{-1}$ , interrupted by longer quiescent phases. As mentioned in Section 1, episodic accretion seems to provide the most consistent explanation for current observations of protostars, while a short ( $\sim 10^4$  yr) accretion phase based on previous estimates of class 0 lifetimes, with accretion rates significantly decreasing during the subsequent class I phase, seems to be ruled out (Enoch et al. 2009; Evans et al. 2009). Several theoretical scenarios have been suggested to explain phases of non-steady accretion (Kenyon & Hartmann 1995; Vorobyov & Basu 2005; Zhu et al. 2009; Tassis & Mouschovias 2005). We adopt here a burst mode as suggested by Vorobyov & Basu (2005) to explore the effect of episodic accretion on the structure of proto-stars/BDs. We assume an arbitrary number of bursts,  $N_{\text{burst}}$ , with typical accretion rate  $\dot{M}_{\text{burst}} \geq 10^{-4} M_{\odot} \text{ yr}^{-1}$  and duration  $\Delta t_{\text{burst}} \sim 100$  yr, interrupted by quiescent phases of duration  $\Delta t_{\text{quiet}} = 1000$ – $5000$  yr (see Vorobyov & Basu 2005). During the quiescent phases, we adopt  $\dot{M} = 0$  as a simplification.<sup>4</sup> We have explored two possibilities for the beginning of the burst phase (cases (a) and (b) described in Table 2). The results are displayed in Figure 3. The burst phases are characterized by evolutionary tracks which follow an erratic behavior with abrupt variations of  $L$  and  $T_{\text{eff}}$ . Our calculations show that, depending on  $m_i$ ,  $N_{\text{burst}}$ , and  $\dot{M}_{\text{burst}}$ , it is possible to populate the region in the H–R diagram after  $\sim 1$  Myr or less between the (non-accreting) 1 Myr and 10 Myr isochrones, producing a natural spread in luminosity. For values of  $\dot{M}_{\text{burst}} \geq 10^{-4} M_{\odot} \text{ yr}^{-1}$ , the evolution is severely affected, while for smaller rates the structure is only moderately affected and the object has time to relax once episodic accretion stops, having properties at  $\sim 1$  Myr similar to the non-accreting counterpart of same mass and age. This is illustrated by case 4(a) (see Table 2) in Figure 3 (cyan dotted curve), with  $\dot{M}_{\text{burst}} = 10^{-5} M_{\odot} \text{ yr}^{-1}$ . Similar evolutionary properties are obtained adopting case (a) or (b) for the beginning

<sup>4</sup> Adopting rates  $\dot{M} < 10^{-6}$  provides the same qualitative results and does not affect our conclusions.

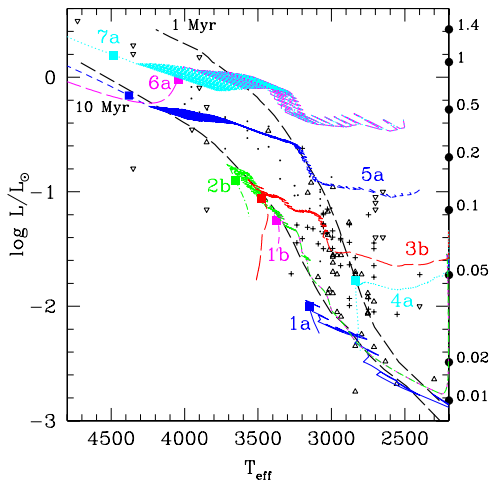


**Figure 3.** Evolutionary sequences in an H-R diagram with episodic accretion. The labels close to each colored curve correspond to the cases described in Table 2. Symbols and other curves are the same as in Figure 1.

of the burst phase. The duration of the quiescent phase  $\Delta t_{\text{quiet}}$  is found to be inconsequential and can be increased from  $10^3$  yr to  $\sim 10^4$  yr without significant effects. This reflects the fact that the thermal timescale of the accreting object rapidly exceeds values  $\gg 10^4$  yr. The contracting object has thus no time to relax to a larger radius state for its new mass if quiescent phases last less than  $10^4$  yr. For typically 10–100 burst episodes, this means that episodic accretion can last a few  $10^5$  yr, in agreement with recent revised estimates of class 0 and class I lifetimes (Enoch et al. 2009; Evans et al. 2009).

#### 4. DISCUSSION AND CONCLUSION

The main results presented in Section 3 can be summarized as follows: (1) for  $\alpha = 0$ , an accreting object has a more compact structure at  $\sim$  a few Myr, i.e. a smaller radius and thus a smaller luminosity, looking older, than the non-accreting counterpart of same mass and age; (2) if a fraction of the accretion energy is absorbed by the protostar interior ( $\alpha \neq 0$ ), this extra energy source partly compensates or, for  $\alpha \gtrsim 0.2$  (assuming  $\epsilon=1/2$ ), even dominates the contraction due to mass accretion, leading in the latter case to a larger radius than the non-accreting object of same mass and age. Our results show that a scenario based on early stages of non-steady accretion, characterized by short duration (a few 100 yr) episodes of vigorous accretion ( $\dot{M} \sim 10^{-4} M_{\odot} \text{ yr}^{-1}$ ), followed by longer quiescent ( $\dot{M} \lesssim 10^{-5} M_{\odot} \text{ yr}^{-1}$ ) phases, naturally produces a spread in the H–R diagram at ages of  $\sim$  a few Myr, provided non-spherical accretion (through disk or funnels) occurs on a variety of proto-star/BD initial masses, from a few  $M_{\text{Jup}}$  to a few tenths of  $M_{\odot}$ . This scenario can easily produce a luminosity spread equivalent to an age spread of  $\sim 10$  Myr (for non-accreting objects), even though the objects are just 1 or so Myr old. We find that such a spread can be obtained if only a negligible amount of the accretion energy contributes to the contracting object’s internal energy ( $\alpha \ll 1$ ), i.e. if most of the accreting kinetic energy is radiated away.

Our scenario, however, cannot explain the observed population of very luminous low-mass objects, which lie largely above the 1 Myr non-accreting isochrone, as displayed in Figures 1 and 3. As discussed in Section 3.1, calculations with  $\alpha \neq 0$  cannot maintain luminous objects at ages of  $\sim$  Myr, with accretion rates consistent with the observed ones at this age, because of

the too short thermal timescale. It thus seems difficult to explain the luminosity of these objects with accretion. A possible explanation is that they are significantly younger ( $\ll 1$  Myr) than the mean cluster age and experienced their episodic accretion phase quite recently. Another explanation, as discussed in Chabrier et al. (2007), is that fast rotation and/or the presence of a magnetic field yields a smaller heat flux output, thus (1) a larger radius and (2) a cooler  $T_{\text{eff}}$ , while barely affecting the luminosity, for a given mass. The net effect would be to shift the location of  $\sim 1$  Myr old objects of a given mass at cooler  $T_{\text{eff}}$  for a given  $L$ , and thus on the right side of the 1 Myr non-accreting isochrone. Note that this may apply as well to the other (hotter) objects, even though there is no need to invoke such a process to reproduce their luminosity. This suggestion should motivate observational determinations of the rotation velocity and the level of magnetic activity of these overluminous objects. The present analysis supports the conclusion of Mohanty et al. (2009) on the origin of the  $T_{\text{eff}}$  reversal in the young eclipsing binary BD 2M0535–05, which excludes an explanation based on prior accretion. At last, another explanation for the location of these objects in the H–R diagram is a less reliable photometry. All the overluminous objects in the Peterson et al. (2008) sample, for instance, are located in a region of the Orion Molecular Cloud with very high nebulosity (D. Peterson 2008, private communication).

The suggestion, as explored in this Letter, that episodic accretion provides a plausible explanation for the observed spread in H–R diagrams at ages of a few Myr (see Section 1) is supported by recent observations of protostars (Enoch et al. 2009; Evans et al. 2009). Furthermore, our predicted significant spread in radius at ages of  $\sim$  Myr (see Figure 2) is consistent with the recently suggested existence of such a spread in the ONC, based on the rotation periods and projected radial velocities of low-mass objects (Jeffries 2007). Episodic accretion thus seems to provide several matching pieces to the puzzle describing the early evolution of LMS and BDs. If our suggestion is correct, it has several drastic consequences: (1) what was interpreted as a significant age spread in SFRs or young clusters is essentially a spread in radius, thus in luminosity, for objects of comparable ages; (2) if young low-mass objects have experienced strong episodes of accretion during their embedded (class 0 to I) phase, their contraction proceeds very differently from a standard, constant  $T_{\text{eff}}$ , Hayashi track and still keep memories of these early episodes after about a few Myr, even if present accretion rates are negligible; (3) trying to infer the mass, thus an initial mass function (IMF), for young ( $\lesssim$  Myr old) clusters from mass–luminosity or mass– $T_{\text{eff}}$ –Sp type relationships based on non-accreting objects/models very likely leads to results of low significance, and inferring the IMF for such young associations seems to be elusive. At this stage, determination of the proto-star/BD core mass function (CMF) with submillimeter surveys will bring more robust information about the star formation process and the stellar mass spectrum (see, e.g., Hennebelle & Chabrier 2008, 2009). Finally, the present calculations show that the concept of a stellar birthline has no real significance, at least for low-mass objects, as the first appearance of these objects in a H–R diagram is very random due to the variety of prior accretion histories.

We thank D. Peterson and A. Natta for providing tables of their data, K. Luhman, D. Peterson, S. Mohanty, A. Scholz, and R. Jayawardhana for valuable discussions. I.B. and G.C. thank the astronomy department of the University of St Andrews

for hospitality. This work was supported by the Constellation network MRTN-CT-2006-035890 and the French ANR MAPP project.

## REFERENCES

- Ballesteros-Paredes, J., & Hartmann, L. 2007, *RevMexAA*, **43**, 123  
Baraffe, I., Chabrier, G., Allard, F., & Hauschildt, P. H. 1998, *A&A*, **337**, 403  
Chabrier, G., & Baraffe, I. 1997, *A&A*, **327**, 1039  
Chabrier, G., Gallardo, J., & Baraffe, I. 2007, *A&A*, **472**, L17  
Dunham, M. M., et al. 2008, *ApJS*, **179**, 249  
Enoch, M. L., Evans, N. J., Sargent, A. I., & Glenn, J. 2009, *ApJ*, **692**, 973  
Evans, N. J., et al. 2009, *ApJS*, **181**, 321  
Gallardo, J., Baraffe, I., & Chabrier, G. 2009, *A&A*, submitted  
Gatti, T., Natta, A., Randich, S., Testi, L., & Sacco, G. 2008, *A&A*, **481**, 423  
Gatti, T., Testi, L., Natta, A., Randich, S., & Muzerolle, J. 2006, *A&A*, **460**, 547  
Hartmann, L. 2001, *AJ*, **121**, 1030  
Hartmann, L., Cassen, P., & Kenyon, S. J. 1997, *ApJ*, **475**, 770  
Herczeg, G. J., & Hillenbrand, L. 2008, *ApJ*, **681**, 594  
Hennebelle, P., & Chabrier, G. 2008, *ApJ*, **684**, 395  
Hennebelle, P., & Chabrier, G. 2009, *ApJ*, in press  
Hillenbrand, L. 2009, in *IAU Symp. 258, The Age of Stars*, ed. E. Mamajek, et al. (Cambridge: Cambridge University Press), 81  
Jeffries, R. D. 2007, *MNRAS*, **381**, 1169  
Kenyon, S. J., & Hartmann, L. 1995, *ApJ*, **101**, 117  
Kenyon, S. J., Hartmann, L., Strom, K. M., & Strom, S. E. 1990, *AJ*, **99**, 869  
Mohanty, S., Jayawardhana, R., & Basri, G. 2005, *ApJ*, **626**, 498  
Mohanty, S., Stassun, K. G., & Mathieu, R. 2009, *ApJ*, **697**, 713  
Muzerolle, J., et al. 2005, *ApJ*, **625**, 906  
Myers, P. C., et al. 1998, *ApJ*, **492**, 703  
Peterson, D., et al. 2008, *ApJ*, **685**, 313  
Siess, L., et al. 1997, *A&A*, **326**, 1001  
Tassis, K., & Mouschovias, T. C. 2005, *ApJ*, **618**, 769  
Vorobyov, E. I., & Basu, S. 2005, *ApJ*, **633**, L137  
Young, C. H., & Evans, J. E. 2005, *ApJ*, **627**, 293  
Zhu, Z., Hartmann, L., & Gammie, C. 2009, *ApJ*, **694**, 1045